ELSEVIER

Journal of Nuclear Materials 313–316 (2003) 828–833

journal of nuclear materials

www.elsevier.com/locate/jnucmat

Influence of plasma–wall interactions on the behaviour of ELMs in JT-60U

A.V. Chankin *, N. Asakura, T. Fukuda, A. Isayama, K. Itami, Y. Kamada, H. Kubo, Y. Miura, T. Nakano, N. Oyama, S. Takeji, H. Takenaga

Japan Atomic Energy Research Institute, Naka-machi, Naka-gun, Ibaraki-ken 311-0193, Japan

Abstract

In JT-60U, extensive plasma–neutral interaction during type I edge localized modes (ELMs) leads to a transient increase in the edge plasma density, seen as spikes of a few ms duration on the inner vertical interferometer channel (FIR1). The spikes can reach up to ~40% of the pre-ELM level of the FIR1 signal, in the case of giant ELMs. Fast edge measurements revealed that these density spikes are caused by ionisation of neutrals circulating between the plasma and the wall, as a result of the ELM particle and heat load onto the target. The increase in the edge density is more or less equally divided between the scrape-off layer (SOL) and outer core region, but is outside of the top of the H-mode pedestal. Prompt ionisation of neutrals and the increase in the plasma density around the separatrix position may affect the edge MHD stability, as often manifested by the occurrence of a second, satellite ELM triggered at lower pedestal temperature and pressure, clusters of type III ELMs or periods of L-mode. Both the magnitude of the density spikes and the observed changes in the ELM behaviour were found to depend on the wall conditions.

PACS: 52.40H
Keywords: Plasma-wall interactions; Divertor; ELM; Scrape-off layer; Separatrix; Recycling

1. Introduction

Edge localized modes (ELMs) are a periodic MHD instability at the plasma edge found in the H-mode and triggered by a critical edge pressure gradient. They result in plasma particle and energy expulsion from the edge causing enhanced recycling and D_α emission [1]. In principal, ionisation of neutrals released from the surrounding surfaces, may lead to partial compensation for the number of lost particles from the plasma during an ELM. When these surfaces are saturated with deuterium, its release and ionisation after the exposure by heat and particle fluxes caused by ELMs might even lead to a transient or long-lasting increase in the plasma density. In JT-60U, this appears to be a typical situation with type I ELMs. It has been found that almost after every type I ELM in this machine there is a transient (and sometimes long-lasting) increase in the plasma density measured by the inner vertical far infrared interferometer chord FIR1, shown in Fig. 1. A giant ELM (large type I ELM preceded by an ELM-free period), can also cause a density increase on the outer channel, FIR2. So far, no correlation between the size of density spikes on the FIR1 signal and the magnetic geometry was found, but strong correlation with the wall conditions has been observed. Similar spikes have been earlier reported on DIII-D [2], where they were attributed to the broadening of the SOL. In the case of JT-60U, experimental evidence presented below clearly demonstrates that these density spikes also affect the plasma inside the separatrix and they have wider implications for the overall plasma behaviour. No such spikes have

* Corresponding author. Tel.: +81-29 270 7530; fax: +81-29 270 7459.
E-mail address: alexch@fusion.naka.jaeri.go.jp (A.V. Chankin).

0022-3115/03/$ - see front matter
PII: S0022-3115(02)01458-7

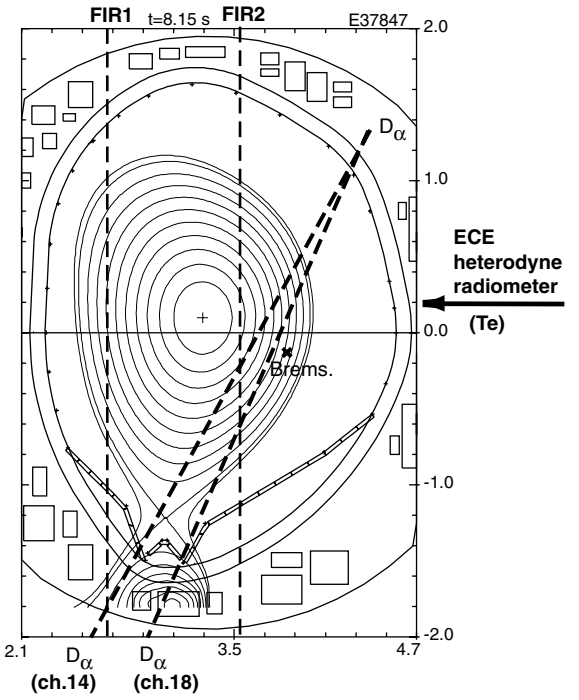

Fig. 1. Plasma shape and diagnostic arrangement for the shot E37847.

been reported from JET (see e.g., a dedicated study on the giant ELM interaction with the divertor target in JET [3]), although their existence in some plasmas following the first giant ELM in the discharge has been communicated orally by the first author of [3].

2. Experimental results

Fig. 1 shows the magnetic geometry of a dedicated type I ELMy discharge used for fast ELM analysis, together with the location of the two available FIR chords (measuring line integral of plasma electron density, n_e), two D_α channels used to monitor neutral flux in the divertor, position of ECE heterodyne radiometer channels (used for electron temperature, T_e, measurements) and the tangency point of an edge channel of the horizontal tangential array measuring visible Bremsstrahlung radiation (Brems.). The toroidal field and plasma current were $Bt/Ip = 3.8T/1.9$ MA. No gas puffing was used in the divertor phase of this discharge, and the density was maintained by positive NBI power of ~20 MW. Fast data inside a 365 ms time window are presented in Fig. 2(a). Each ELM coincides with a significant (~6%, on average) increase in the line average density, $\bar{n}_e$, measured by the interferometer chord FIR1. No such spikes can be seen on the FIR2 channel, whose chord is closer to the plasma centre, but sharp spikes are also observed

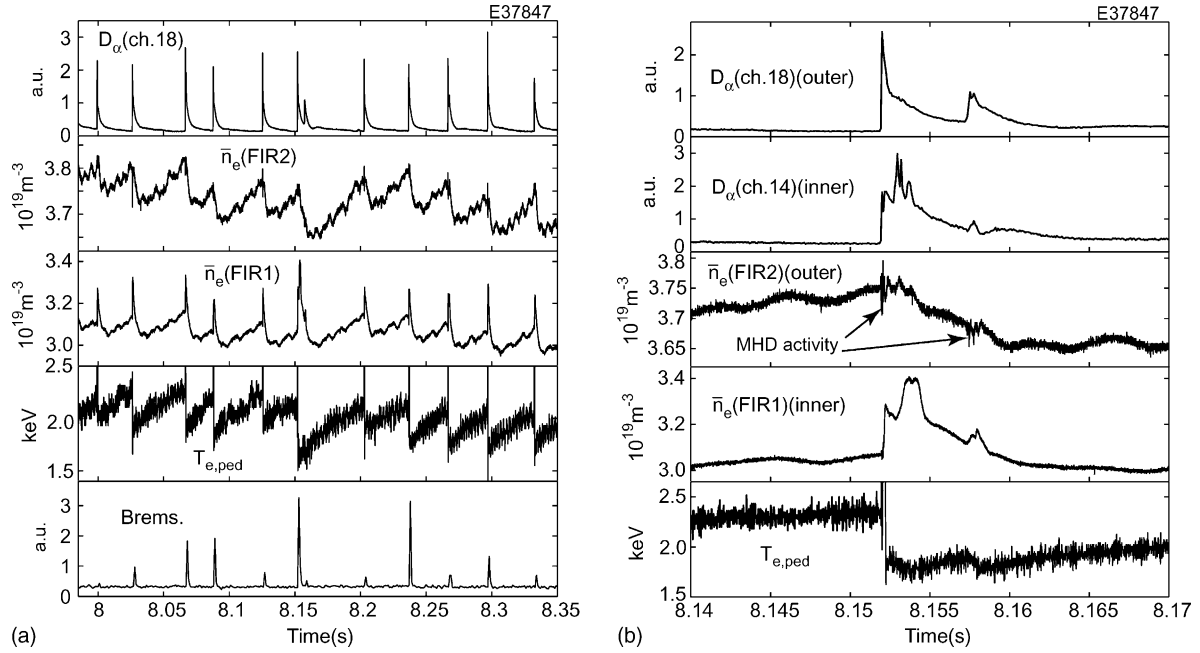

Fig. 2. (a) D_α emission from the channel 18 viewing the outer strike point in the divertor, $\bar{n}_e$ measured by the outer (FIR2) and inner (FIR1) interferometer chords, T_e at the H-mode pedestal, $T_{e,ped}$, and edge visible Bremsstrahlung emission, for the shot E37847. (b) D_α emissions from channels 18 and 14, $\bar{n}_e$ measured by FIR2 and FIR1 channels of the interferometer, and pedestal electron temperature $T_{e,ped}$, for the narrow time window of the shot E37847.

on the edge Bremsstrahlung channel, indicating that the density rise is not an in-out asymmetric phenomenon, favouring only the high field side.

Fig. 2(b) presents fast data inside a narrower time window for the ELM in the middle of the time window of Fig. 2(a), which caused the largest drop in the pedestal electron temperature, $T_{e,ped}$. Edge T_e and n_e profiles, measured before and after this ELM, are presented in Fig. 3. They exhibit very little changes in the edge n_e, including the region near the pedestal top, against almost complete erosion of the T_e pedestal. This feature of density profiles is typical of the ELM behaviour in JT-60U. It shows that the large, ~10%, $\bar{n}_e$ rise, observed on the FIR1 (Fig. 2(b)), should be attributed mainly to the density increase in more outer layers, closer to the separatrix. Shortly after the large ELM at 8.144 s, another, small (satellite) ELM occurred at 8.157 s, during the phase of increased D_α radiation caused by the main ELM. Since it occurred at much lower $T_{e,ped}$ and electron pressure, $p_{e,ped}$, than other ELMs in this discharge, one has to conclude that it was triggered by some changes in the outer layers of the plasma, outside of the pedestal top, where prompt ionisation of neutrals has caused the density rise (see below). Both ELMs, shown in Fig. 2(b), are accompanied by bursts of large-scale density oscillations on FIR2. The duration of such oscillations was about the same as the duration of Mirnov probe oscillations observed during the MHD phase of the ELM. These density oscillations, which probably are caused by the ballooning nature of the ELM crash (MHD activity localised at the low field side), were found instrumental in determining the duration of the MHD phase of ELMs in JT-60U [4].

An example of a discharge with one of the largest spikes on the FIR1 channel observed in JT-60U is presented in Fig. 4. A staggered rise of the NBI power from 5 to 15 MW has caused a series of giant ELMs in this $Bt/Ip = 3.8$ T/2 MA discharge with the magnetic geometry similar to the one shown in Fig. 1. The relative increase in the FIR1 signal after the first giant ELM was 44%. This ELM has also caused an increase in the FIR2 signal by 13%. Despite that, YAG Thomson measurements did not reveal any appreciable changes in the pedestal n_e, within the error bars of ~15%, implying that the main density increase has occurred outside of the pedestal top. Each giant ELM in this discharge has triggered clusters of type III ELMs of ~100 ms duration. The first three clusters gave way to ELM-free periods with further rising $T_{e,ped}$, after the chordal density, measured by FIR channels, edge visible Bremsstrahlung radiation and the background D_α emission fell back close to their pre-ELM levels (except for the first giant ELM, where the D_α emission fell to about twice its

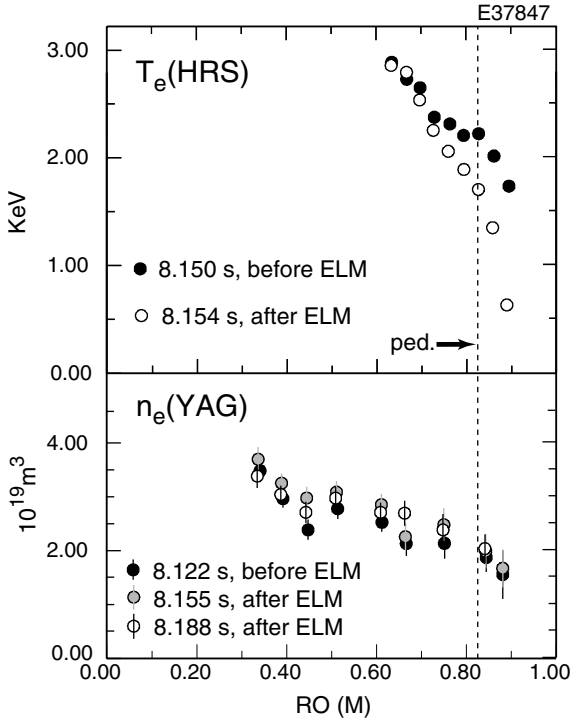

Fig. 3. Electron temperature and density profiles before and after the ELM shown in Fig. 2(b), measured by the heterodyne radiometer system (T_e) and YAG Thomson scattering (n_e).

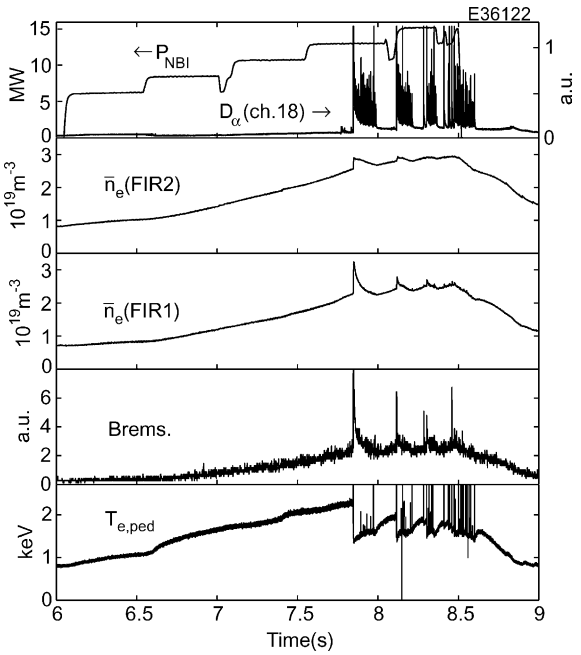

Fig. 4. NBI input power, D_α emission from the channel 18, $\bar{n}_e$ measured by the interferometer (FIR2 and FIR1 chords), and edge visible Bremsstrahlung emission, for the shot E36122.

pre-ELM level). At the times of type III ELMy to ELM-free phase transitions, the $T_{e,ped}$ was close to its level just after the giant ELMs (and for third such transition – right at this level). One should therefore conclude that it is the increased level of the plasma–wall interaction and the rise in the extreme edge density, rather than the increased pedestal collisionality, which was responsible for type III ELMy periods.

To pinpoint the exact location of density rise during type I ELMs, dedicated experiments with the horizontal plasma sweep have been conducted, with the position of the FIR1 chord sweeping through the SOL, pedestal and core regions. The results are presented in Fig. 5, for three ELMs under the conditions where the tangency point of the FIR1 chord was inside of the pedestal, at the separatrix and in the SOL. Following the procedure described in [5], the plasma edge was divided into three density regions: SOL, pedestal (from the top of the pedestal up to the separatrix) and inside the pedestal, in order to evaluate the contribution at each radial position to the increase in the line-integrated density of FIR1. Then, each contribution was simply estimated beginning from the SOL towards the inside the pedestal region by fitting the sum of density increase of line-integrated density taking into account the integration length of each region. As a result, it has been established that the increase in the density, δn_e, following an ELM is more or less equally spread between the SOL and the pedestal region. At the same time, δn_e in the core region was less than 15% of the previous two, with the relative increase in density less than 10% of its average in the other two zones. The steep pedestal density gradient is thus being partially filled in by the increase in the plasma density around the separatrix position. In these and other

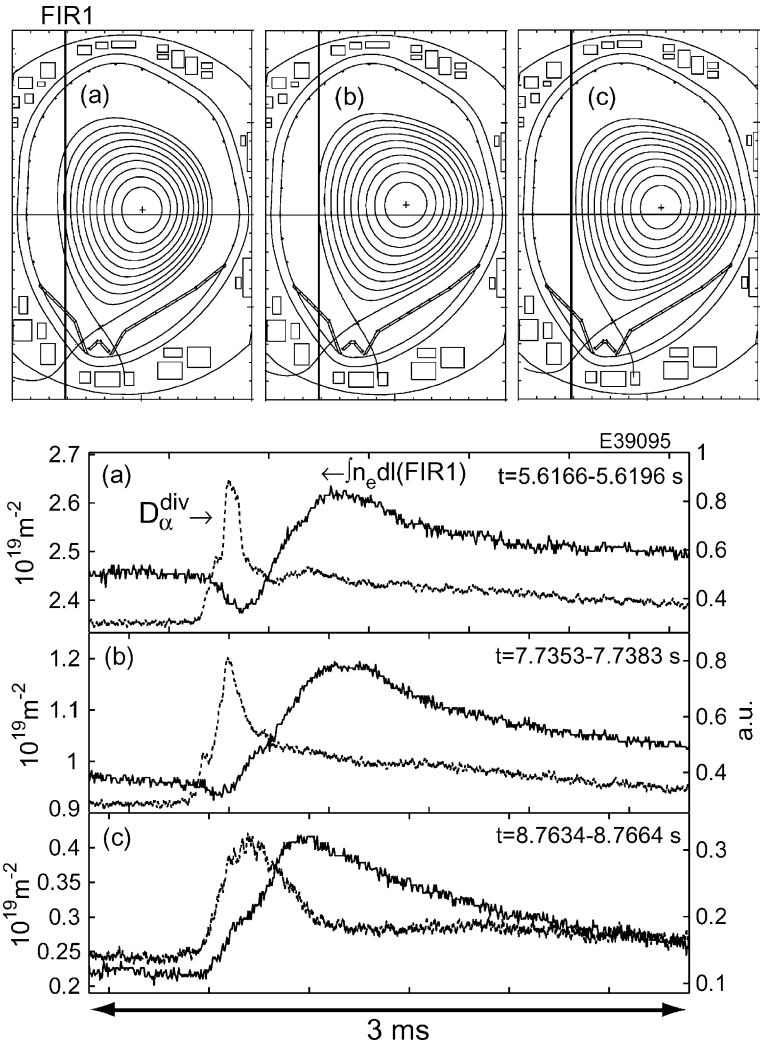

Fig. 5. Details of the experiment with horizontal sweeps of the plasma.

experiments with fast edge measurements it has also been confirmed that the rise in the divertor D_α emission always precedes the rise in the FIR1 signal. In Fig. 5, the line integrated density in configurations (a) and (b) first shows a small drop, which was explained as the result of a large density drop ('density collapse') during the ELM crash at the outer, low-field side, prompting parallel plasma flow from the inside to the outside with the ion sound speed to fill the emerged density 'hole' [5]. However, the poloidal size of this hole (that is, the poloidal extent of the 'density collapse') is small [5].

Influence of wall conditions on the magnitude of the FIR1 spikes and the behaviour of ELMs is demonstrated in Fig. 6. The two discharges shown have been performed in the same magnetic configuration with $Bt/Ip = 3T/1.8$ MA. In this series of experiments, aimed at clarification of the effect of neutrals on the L–H power threshold (see results in [6]), wall conditions have been continuously improving as a result of pumping, in the absence of the gas puffing (only NBI injection fuelling was used). The two shots presented in Fig. 6 have been performed almost at the very beginning (E33631) and at the end (E33677) of this series of shots. During the flat-top phases, shown on the figure, the first discharge had input power $P_{NBI} = 16.7$ MW, radiated power $P_{rad} = 5.5$ MW, stored energy $W_{dia} = 3.55$ MJ and line average density (along FIR2 chord) $\bar{n}_e = 3.1 \times 10^{19}$ m^{-3}. The second discharge had $P_{NBI} = 12.6$ MW, $P_{rad} = 6.5$ MW, $W_{dia} = 2.9$ MJ and $\bar{n}_e = 3.85 \times 10^{19}$ m^{-3}. Higher density in the second shot, with lower input power, must be caused by better particle confinement at the edge, since the FIR1 signal shows continuous rise in between ELMs. The FIR1 signal reveals more regular ELMs with the density spikes of ~3% in the case of the second shot, performed on cleaner walls. Whereas in the first shot, each ELM was followed by one or two smaller ELMs, with the average increase on the FIR1 signal of ~8%. Neutral desorption from deuterium-saturated walls and subsequent ionisation was apparently responsible for higher chordal density after the ELM than before the ELM, for the majority of large ELMs in the first shot.

Another example of the influence of wall conditions on the ELM behaviour is presented in Fig. 7. The two discharges had the same magnetic configuration, similar to the one shown in Fig. 5 (case C), with $Bt/Ip = 2.5$ T/1.2 MA. The first discharge was performed at $P_{NBI} = 13$ MW on well conditioned wall, as a result of many preceding NBI shots, and the second – on the wall not yet conditioned by the NBI, at $P_{NBI} = 11$ MW. Larger FIR1 spikes during ELMs are observed in the second shot, with transitions to the L-mode following

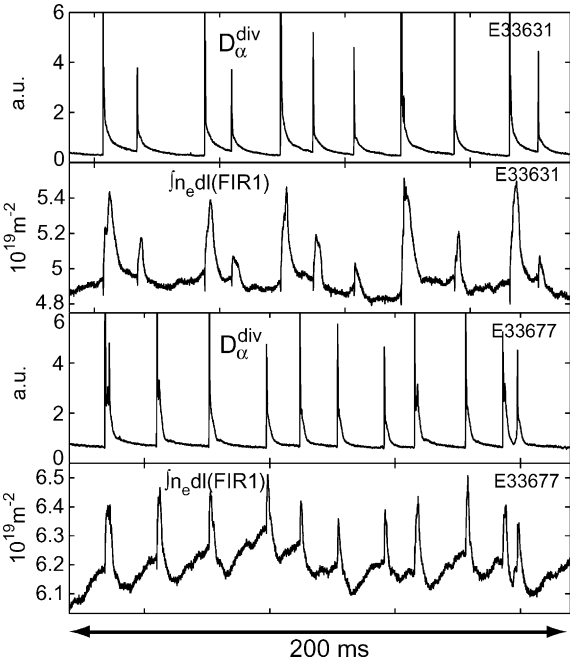

Fig. 6. D_α emission from the divertor (channel 18 used) and line integral of electron density along the FIR1 chord, for the two shots with the same magnetic geometry but different wall conditions: shot E33677 was the last in the long series of shots with pumping.

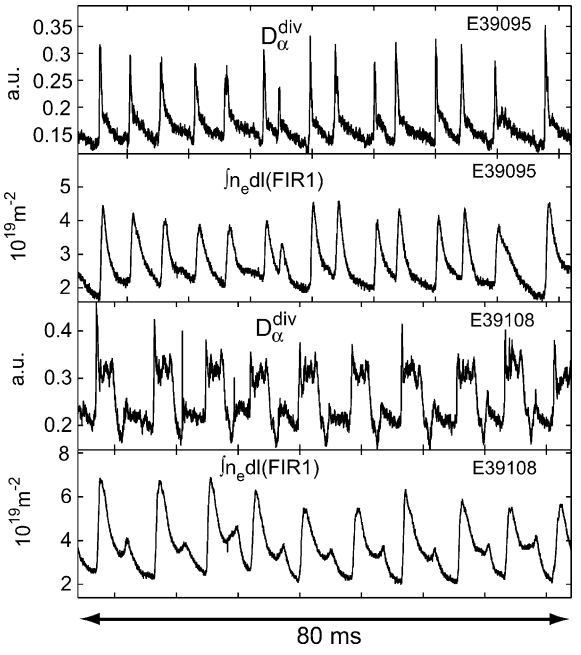

Fig. 7. D_α emission from the divertor (channel 18 used) and line integral of electron density along the FIR1 chord, for the two shots with the same magnetic geometry: E39095 – wall well conditioned by NBI discharges, E39108 – poorly conditioned wall.

each ELM. It was also observed that back HL transitions after large ELMs have not been eliminated by lowering recycling by reducing the wall temperature from 300 to 150 °C, which again emphasises the importance of surface layers, subjected to plasma particles and neutrals bombardment during ELMs, for the ELM behaviour.

3. Discussion and conclusions

It is widely accepted that type I ELMs are closely connected with normalised local edge pressure gradients near the ideal ballooning limit, determined by the plasma parameters at the H-mode pedestal [7]. This must be true for ELMs which are preceded by periods of relatively low interaction with walls (either inter-ELM periods of the duration sufficient for the relaxation after ELMs or ELM-free periods). At the same time, experimental results from JT-60U presented here indicate the importance of the extreme edge, outside of the pedestal top, and plasma–wall interactions for the behaviour of subsequent ELMs. Contrary to the general perception, type I ELMs in JT-60U typically result in higher edge density just after an ELM (at least transiently), due to an apparent excess of the ionisation of desorbed neutrals in the extreme edge over the direct loss of charged particles as a result of the MHD activity. These changes in the extreme edge are capable of triggering smaller, satellite ELMs, clusters of type III ELMs, or L-mode periods under conditions at the pedestal which may not warrant the ELM onset. Such influence of plasma–wall interactions on the ELM behaviour is strongly affected by wall conditions, where the important role must be played by surface layers saturated with the working gas.

The results presented here are not necessarily in contradiction with edge stability analysis. At present, coupled peeling–ballooning modes, where the pedestal current density plays an important role, are considered as possible candidates to explain type I ELMs (see e.g., [8]). Details of the edge profiles up to the separatrix, influenced by the plasma–wall interaction (in particular, the evolution of the Bootstrap current inside the pedestal region) have to be taken into account by the edge stability models, to analyse their impact on the ELM behaviour.

References

[1] H. Zohm, Plasma Phys. Control Fusion 38 (1996) 105.
[2] R.A. Jong, G.D. Porter, R.J. Groebner, C.J. Lasnier, G.A. Thomson, Plasma Phys. Control Fusion 38 (1996) 1381.
[3] J. Lingertat, A. Tabasso, S. Ali-Arshad, et al., J. Nucl. Mater. 241–243 (1997) 402.
[4] A.V. Chankin, N. Asakura, T. Fukuda, A. Isayama, Y. Kamada, Y. Miura, N. Oyama, S. Takeji, H. Takenaga, Fast ELM Dynamics in JT-60U, Nucl. Fusion 42 (2002) 733.
[5] N. Oyama, Y. Miura, A.V. Chankin, H. Takenaga, N. Asakura, Y. Kamada, T. Oikawa, K. Shinohara, S. Takeji, Asymmetry of collapse of density pedestal by type I ELM on JT60U, presented at 8th IAEA Technical Committee Meeting on H-Mode Physics and Transport Barriers, 5–7 September, NIFS, Toki, Japan, Nucl. Fusion, submitted for publication.
[6] T. Fukuda, T. Takizuka, K. Tsuchiya, Y. Kamada, N. Asakura, Plasma Phys. Control Fusion 42 (2000) A289.
[7] ITER Physics Basis, Nucl. Fusion 39 (1999) 2298.
[8] L.L. Lao, P.B. Snyder, J.R. Ferron, et al., 29th EPS Conference on Plasma Physics and Control Fusion, Montreux 17–21 June 2002, ECA vol. 26B, P-1.091, 2002.